AN IMPROVED QUADRATURE RULE FOR THE FLUX-COMPUTATION IN HIGH-RESOLUTION NONOSCILLATORY CENTRAL DIFFERENCE SCHEMES FOR SYSTEMS OF CONSERVATION LAWS IN MULTIDIMENSIONS

KNUT–ANDREAS LIE AND SEBASTIAN NOELLE

ABSTRACT. We present a new second-order, nonoscillatory, central difference scheme on two-dimensional, staggered, Cartesian grids for systems of conservation laws. The scheme uses a new, carefully designed integration rule for the flux computations and thereby takes more propagation directions into account. This effectively reduces grid orientation effects produced for two-dimensional radially symmetric gas flows and improves the accuracy for smooth solutions.

1. INTRODUCTION

Consider systems of hyperbolic conservation laws

$$u_t + f(u)_x + g(u)_y = 0, \qquad u(x,0) = u_0(x), \tag{1}$$

where $u : \mathbb{R}^2 \times \mathbb{R}_+ \to \mathbb{R}^m$ is the vector of conservative variables and $f, g : \mathbb{R}^m \to \mathbb{R}^m$ are the fluxes in x- and y-direction. Prototypes of these equations are the Euler equations of gas dynamics, the shallow water equations, and the equations of ideal magnetohydrodynamics, to name a few.

Nonoscillatory, central difference schemes as introduced by Nessyahu and Tadmor [1] have proved to be efficient computational methods for systems of conservation laws. Since the schemes apply no characteristic information or Riemann solvers, they yield especially compact and simple computer code and can easily be applied to systems for which no Riemann solver exists.

The Nessyahu–Tadmor scheme was extended to two spatial dimensions in [2, 3]. This two-dimensional scheme (abbreviated hereafter NT2d) has been called truly multidimensional since it does not use one-dimensional characteristic decompositions. We will review the scheme with special emphasis on the quadrature rules for the fluxes across the boundaries of the cells. The fluxes are evaluated in the corners of the cells, which lie in the interior of cells in the staggered dual grid. The fluxes computed into the x- and y-directions add up to a single flux into the diagonal direction, and only these two diagonal directions are effectively used in the NT2d scheme. We present a radially symmetric explosion problem in gas dynamics for which the scheme clearly produces grid orientation effects. This motivates the derivation of a new staggered scheme that takes twice as many propagation directions into account. This is achieved by introducing a carefully designed integration rule for the flux computations. The new scheme has less grid orientation effects and preserves symmetries better than the original scheme at the expense of a slightly higher runtime. This is demonstrated for the radially symmetric test problem, for which (almost) all directional effects are eliminated.

Date: Submitted to Journal on Scientific Computing. August 17, 2001.

Moreover, the new scheme gives decreased errors and improved convergence rates for a test case of oblique, linear advection.

2. Flux Computations in the two-dimensional Nessyahu–Tadmor Scheme

Define the points in a regular Cartesian grid by $x_j = j\Delta x$, $y_k = k\Delta y$ and $t_n = n\Delta t$, $j,k \in \mathbb{Z}$, $n \in \mathbb{N}$. The NT2d scheme approximates cell-averages of the solution on two sets of grids, the *original* and the *staggered*, respectively:

$$C_{j,k} = [x_{j-\frac{1}{2}}, x_{j+\frac{1}{2}}] \times [y_{k-\frac{1}{2}}, y_{k+\frac{1}{2}}], \qquad C_{j+\frac{1}{2},k+\frac{1}{2}} = [x_j, x_{j+1}] \times [y_k, y_{k+1}].$$

At even time-steps the solution is given as a piecewise linear function over the *original* grid,

$$\overline{w}(x,y,t_n) = \overline{w}^{\,n}_{jk} + \frac{x-x_j}{\Delta x} w'_{jk} + \frac{y-y_k}{\Delta y} w^{\grave{}}_{jk} \quad \text{for} \;\; (x,y) \in C_{jk}. \tag{2}$$

The values $\overline{w}^{\,n}_{jk}$ are cell-averages and the finite-difference operators $' \approx \Delta x \frac{\partial}{\partial_x}$ and $^{\grave{}} \approx \Delta y \frac{\partial}{\partial_y}$ are realised by piecewise linear reconstructions with standard limiter-functions, which are applied to each component of the vectors.

For the next time step, the NT2d scheme computes the update $\overline{w}^{\,n+1}_{j+1/2,k+1/2}$ at time t_{n+1} over the *staggered* cells as

$$\begin{aligned}
\overline{w}^{\,n+1}_{j+\frac{1}{2},k+\frac{1}{2}} =& \frac{1}{4}\big(\overline{w}^{\,n}_{jk} + \overline{w}^{\,n}_{j+1,k} + \overline{w}^{\,n}_{j+1,k+1} + \overline{w}^{\,n}_{j,k+1}\big) \\
&+ \frac{1}{16}\big(w'_{jk} + w'_{j,k+1} - w'_{j+1,k} - w'_{j+1,k+1}\big) \\
&+ \frac{1}{16}\big(w^{\grave{}}_{jk} - w^{\grave{}}_{j,k+1} + w^{\grave{}}_{j+1,k} - w^{\grave{}}_{j+1,k+1}\big) \\
&- \frac{\lambda}{2}\Big[f(w^{n+\frac{1}{2}}_{j+1,k}) + f(w^{n+\frac{1}{2}}_{j+1,k+1})\Big] + \frac{\lambda}{2}\Big[f(w^{n+\frac{1}{2}}_{j,k}) + f(w^{n+\frac{1}{2}}_{j,k+1})\Big] \\
&- \frac{\mu}{2}\Big[g(w^{n+\frac{1}{2}}_{j+1,k+1}) + g(w^{n+\frac{1}{2}}_{j,k+1})\Big] + \frac{\mu}{2}\Big[g(w^{n+\frac{1}{2}}_{j+1,k}) + g(w^{n+\frac{1}{2}}_{j,k})\Big],
\end{aligned} \tag{3}$$

where $\lambda = \Delta t/\Delta x$, $\mu = \Delta t/\Delta y$, and

$$w^{n+\frac{1}{2}}_{jk} = \overline{w}^{\,n}_{jk} - \frac{\lambda}{2} f'_{jk} - \frac{\mu}{2} g^{\grave{}}_{jk} \tag{4}$$

is a predictor step in the centres of the non-staggered cells at time $t_{n+1/2}$. This predictor step uses the conservation law (1) to approximate the time derivative of w. The odd time-step on the staggered grid is defined analogously, replacing staggered by non-staggered cells and vice-versa.

Let us take a closer look at formula (3). The first three lines on the right-hand-side give the cell-average of the reconstruction $\overline{w}(\cdot, t_n)$ in (2) over the staggered cell $C_{j+\frac{1}{2},k+\frac{1}{2}}$. The following two lines approximate the integral of the fluxes across the boundaries of the cell from time t_n to t_{n+1} by a quadrature rule in space-time. For example, over the western side the space-time quadrature used in (3) is

$$\frac{1}{\Delta y \Delta t}\int_{y_k}^{y_{k+1}}\int_{t_n}^{t_{n+1}} f(w(x_j,y,t))\,dy\,dt \approx \frac{1}{2}\Big(f\big(w^{n+\frac{1}{2}}_{jk}\big) + f\big(w^{n+\frac{1}{2}}_{jk+1}\big)\Big). \tag{5}$$

This quadrature consists of the midpoint rule in time and the trapezoidal rule in space. The nodes of the quadrature rule are (see Figure 2(a) on page 5)

$$(x_j, y_k, t_{n+1/2}), \;\; (x_j, y_{k+1}, t_{n+1/2}). \tag{6}$$

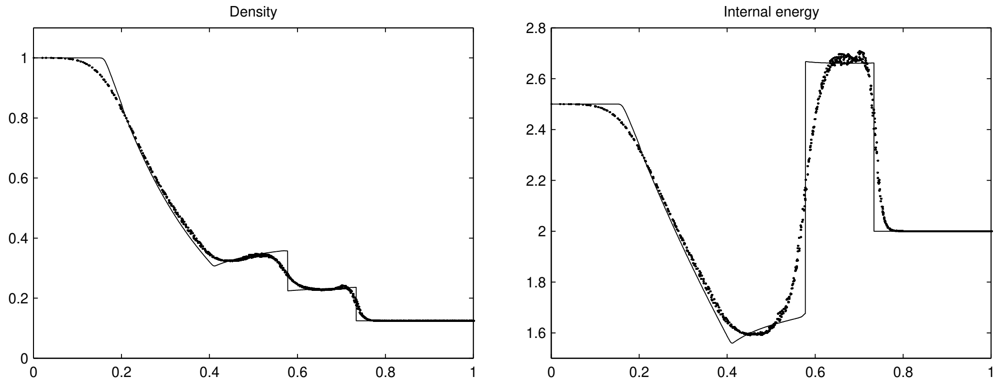

FIGURE 1. Scatter plot of solution at time $t = 0.2$ of the cylindrical explosion problem computed by the original NT2d scheme on a 101×101 grid with WENO limiter and CFL number 0.475.

These points lie on the interface of the *staggered* grid and above the *centres* of the original grid cells. Here the reconstruction (2) is *smooth*. Moreover, the solution of (1) with initial data (2) given at time t_n will remain smooth along $(x_j, y_k) \times [t_n, t_{n+1}]$ as long as the CFL condition

$$\Delta t \ \max\Big(\frac{a_{\max}}{\Delta x}, \frac{b_{\max}}{\Delta y}\Big) < \frac{1}{2} \tag{7}$$

is satisfied. (Here $a_{\max}$ and $b_{\max}$ denote maximal speeds of propagation in the x- and y-directions). It is therefore justified to approximate the solution at $(x_j, y_k,\ t_{n+1/2})$ using Taylor expansions and the conservation law (1) as in (4). As a consequence, no characteristic decompositions of the flux-vectors are needed, which makes the scheme particularly simple to implement. This is the "truly multidimensional" content of the NT2d scheme.

Unfortunately, the scheme sometimes exhibits obvious grid-orientation effects, as will be demonstrated by the following example: Consider the Euler equations for an ideal gas with gas constant $\gamma = 1.4$. Let the initial data be

$$(\rho, u, v, p)(x, y, 0) = \begin{cases} (1.0, 0, 0, 1.0), & |x|^2 + |y|^2 \leq 0.16 \\ (0.0125, 0, 0, 0.1), & \text{otherwise.} \end{cases}$$

The solution consists of a circular shock wave propagating outwards from the origin, followed by a contact discontinuity, and a rarefaction wave travelling towards the origin.

To limit numerical derivatives (as in (2)) we use the smooth WENO limiter

$$\mathrm{WENO}(a, b) = \frac{w(a) \cdot a + w(b) \cdot b}{w(a) + w(b)}, \qquad w(a) = \big(\varepsilon + a^2\big)^{-2},\ \varepsilon = 10^{-6}.$$

Figure 1 shows a scatter plot of the solution at time $t = 0.2$ computed by the original NT2d scheme. In the current setting, a scatter plot for a given physical quantity is a plot of the value in each grid cell versus the distance of the cell centre from the origin. In this way we can present the spread in the data, as a solution with perfect radial symmetry would consist of points lying on a single line.

Although the scheme gives relatively sharp resolution of the shock and the rarefaction wave (the shock is 1–2 computational cells wide for each one-dimensional cross-section of the numerical solution), it suffers from grid orientation effects. This is particularly evident for the internal energy in the zone between the shock and the contact discontinuity. Moreover, overshoots in pressure and radial velocity can be observed behind the leading shock in regions close to the diagonal lines $x = \pm y$.

3. An Improved Quadrature Rule

The presence of grid orientation effects observed in computations on radially symmetric solutions (as demonstrated above, for instance) motivated us to look for a modification of the NT2d scheme that would reduce these directional effects.

Here is our new scheme: We propose to replace (3) by

$$
\begin{aligned}
\overline{w}^{\,n+1}_{j+\frac12,k+\frac12} =& \frac14\big(\overline{w}^{\,n}_{jk} + \overline{w}^{\,n}_{j+1,k} + \overline{w}^{\,n}_{j+1,k+1} + \overline{w}^{\,n}_{j,k+1}\big)\\
&+ \frac{1}{16}\big(w'_{jk} + w'_{j,k+1} - w'_{j+1,k} - w'_{j+1,k+1}\big)\\
&+ \frac{1}{16}\big(w^{\grave{}}_{jk} - w^{\grave{}}_{j,k+1} + w^{\grave{}}_{j+1,k} - w^{\grave{}}_{j+1,k+1}\big)\\
&- \frac{\lambda}{4}\Big[f(w^{n+1}_{j+1,k}) + f^{n,-}_{j+1,k+\frac12} + f^{n,+}_{j+1,k+\frac12} + f(w^{n+1}_{j+1,k+1})\Big]\\
&+ \frac{\lambda}{4}\Big[f(w^{n+1}_{jk}) + f^{n,-}_{j,k+\frac12} + f^{n,+}_{j,k+\frac12} + f(w^{n+1}_{j,k+1})\Big]\\
&- \frac{\mu}{4}\Big[g(w^{n+1}_{j,k+1}) + g^{n,-}_{j+\frac12,k+1} + g^{n,+}_{j+\frac12,k+1} + g(w^{n+1}_{j+1,k+1})\Big]\\
&+ \frac{\mu}{4}\Big[g(w^{n+1}_{jk}) + g^{n,-}_{j+\frac12,k} + g^{n,+}_{j+\frac12,k} + g(w^{n+1}_{j+1,k})\Big],
\end{aligned} \tag{8}
$$

where

$$
w^{n+1}_{jk} = \overline{w}^{\,n}_{jk} - \lambda f'_{jk} - \mu g^{\grave{}}_{jk} \tag{9}
$$

and

$$
\begin{aligned}
f^{n,-}_{j,k+\frac12} =& f(\overline{w}^{\,n}_{jk} + \tfrac12 w^{\grave{}}_{jk}), \qquad & f^{n,+}_{j,k+\frac12} &= f(\overline{w}^{\,n}_{j,k+1} - \tfrac12 w^{\grave{}}_{j,k+1}),\\
g^{n,-}_{j+\frac12,k} =& g(\overline{w}^{\,n}_{jk} + \tfrac12 w'_{jk}), \qquad & g^{n,+}_{j+\frac12,k} &= g(\overline{w}^{\,n}_{j+1,k} - \tfrac12 w'_{j+1,k}).
\end{aligned} \tag{10}
$$

The difference between our new scheme (8)–(10), which we abbreviate LN2d hereafter, and the NT2d scheme (3)–(4) is a new quadrature rule in the computation of the fluxes across the sides. For example, the quadrature rule for the western side corresponding to (5) is now

$$
\frac{1}{\Delta y \Delta t}\int_{y_k}^{y_{k+1}}\int_{t_n}^{t_{n+1}} f(w(x_j,y,t))\,dy\,dt \approx \frac14\Big(f\big(w^{n,-}_{j,k+\frac12}\big) + f\big(w^{n,+}_{j,k+\frac12}\big) + f\big(w^{n+1}_{jk}\big) + f\big(w^{n+1}_{jk+1}\big)\Big). \tag{11}
$$

The nodes of this quadrature rule are (see Figure 2(b)).

$$
(x_j, y_{k+\frac12}, t_n), \quad (x_j, y_k, t_{n+1}), \quad (x_j, y_{k+1}, t_{n+1}).
$$

At the first quadrature point the reconstruction $\overline{w}(\cdot, t_n)$ is now *discontinuous*, so we have to evaluate the fluxes at the *one-sided* limits as in (10).

As long as the CFL condition (7) is satisfied, the quadrature points at time t_{n+1} still lie within the domain of smoothness of the solution to (1) with initial data (2). Therefore it is justified to extrapolate the solution using Taylor series as in (9).

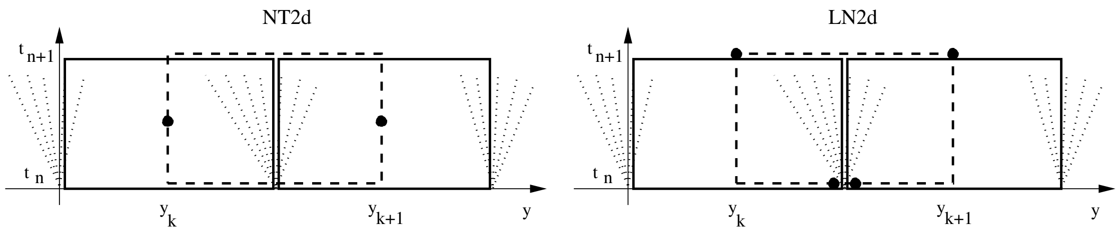

FIGURE 2. Quadrature points for the fluxes over the western side of the staggered grid, shown in the (y,t)-plane. The dashed rectangles are cells of the staggered grid, while the solid rectangles are the sides of the original grid. The dotted lines symbolise Riemann-fans originating from the cell-boundaries of the original grid.

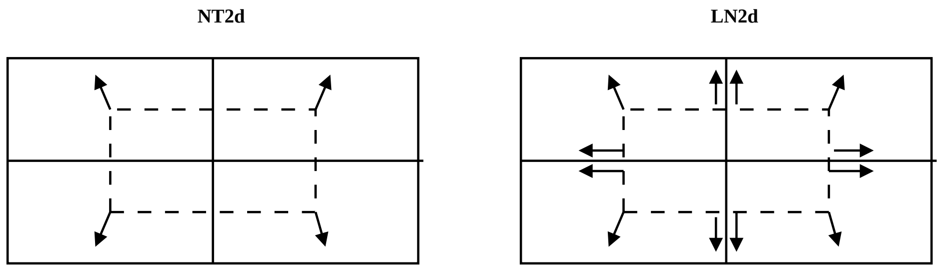

FIGURE 3. Floor-plan of the staggered schemes in the (x,y)-plane. The solid lines symbolise the original cells C_{jk}, the dashed line the staggered cell $C_{j+\frac{1}{2},k+\frac{1}{2}}$, and the arrows the fluxes across its boundaries.

The main advantage of the new quadrature is that it takes *twice as many directions* into account: while the original NT2d scheme effectively uses only the two diagonal directions in the flux computation, LN2d uses the diagonal directions *and* the grid-directions themselves. To see this, let us have a look at the "floorplan" of the two schemes in Figure 3. The NT2d scheme evaluates all fluxes at the corners of the staggered cell. If we multiply (3) by $\Delta x \Delta y / \Delta t$ and collect the fluxes at the quadrature point $(x_{j+1}, y_{k+1}, t_{n+1/2})$ in the north-east corner, we obtain a contribution of

$$\frac{\Delta y}{2} f(w_{j+1,k+1}^{n+\frac{1}{2}}) + \frac{\Delta x}{2} g(w_{j+1,k+1}^{n+\frac{1}{2}})$$

to the flux across the boundary of the cell. This adds up to evaluating the normal flux in the direction

$$n_{\mathrm{NE}} = (\Delta y, \Delta x)/(\Delta x^2 + \Delta y^2)^{\frac{1}{2}}.$$

Similar contributions arise at the north-west, south-west and south-east corners. For a square grid, these are the diagonal directions, and for a general Cartesian grid, the directions normal to the diagonal directions, see Figure 3(a). This leads us to a reinterpretation of the NT2d scheme: rather than evaluating fluxes across the *sides* of the staggered cells, it computes fluxes across its *corners*. The grid directions themselves are not taken into account.

The LN2d scheme (8) uses two sets of quadrature points, those at the old time t_n in the centres of the sides, where fluxes are computed into the grid directions, and those at time t_{n+1} in the corners, where fluxes are computed into the diagonal directions as for the NT2d scheme. Therefore, we now have four directions in two space-dimensions instead of two for

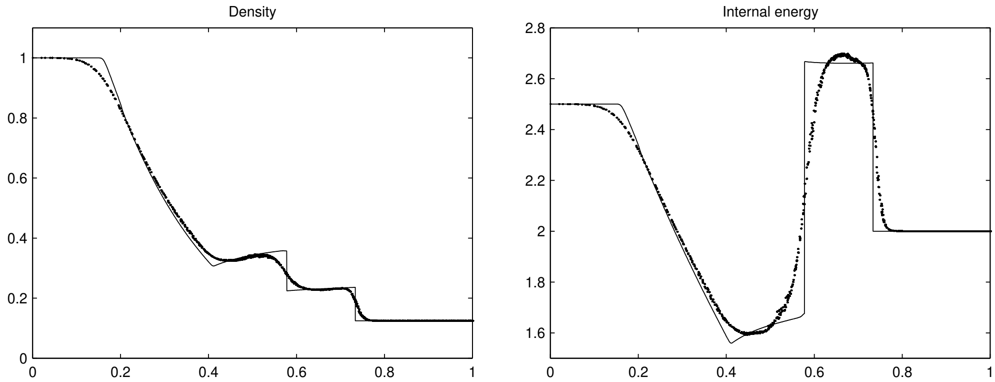

FIGURE 4. Scatter plot of solution at time $t = 0.2$ of the cylindrical explosion problem computed by LN2d on a 101×101 grid with WENO limiter and CFL number 0.475.

the NT2d scheme, see Figure 3(b). As we shall show below, this does reduce grid orientation effects for the radially symmetric flow above.

To obtain more propagation directions, we must pay the price of more flux evaluations, thus making the scheme computationally more expensive. When implemented directly as in (8), twelve flux-evaluations are needed to update a cell instead of two for the NT2d scheme. However, the additional flux-evaluations can be completely avoided by setting

$$f^{n,-}_{j,k+\frac{1}{2}} = f(\overline{w}^{\,n}_{jk}) + \frac{1}{2} f'_{jk} \qquad f^{n,+}_{j,k+\frac{1}{2}} = f(\overline{w}^{\,n}_{j,k+1}) - \frac{1}{2} f'_{j,k+1} \tag{12}$$

and similarly for $g^{n,-}$ and $g^{n,+}$. Equation (12) is exact for linear flux functions. Therefore all additional work needed is to compute f' and g' at time t_n at the centres of the original cells C_{jk}.

Similarly as in [3, Theorem 1], we can prove the following local maximum principle for the new scheme (8), (9), (12):

Theorem 1. *Consider the scheme* (8), (9) *and* (12) *where all discrete derivatives are limited by the MinMod-limiter. Suppose that the CFL-condition*

$$\Delta t \ \max\Big(\frac{a_{\max}}{\Delta x}, \frac{b_{\max}}{\Delta y}\Big) \le C_\theta \tag{13}$$

holds, where the CFL-number C_θ is given by

$$C_\theta = -\frac{2+\theta}{6\,\theta} + \sqrt{\Big(\frac{2+\theta}{6\,\theta}\Big)^2 + \frac{2-\theta}{12\,\theta}}. \tag{14}$$

Then the update $\overline{w}^{\,n+1}_{j+\frac{1}{2},k+\frac{1}{2}}$ satisfies the local maximum principle

$$\min_{j',k'=0,1} \overline{w}^{\,n}_{j+j',k+k'} \le \overline{w}^{\,n+1}_{j+\frac{1}{2},k+\frac{1}{2}} \le \max_{j',k'=0,1} \overline{w}^{\,n}_{j+j',k+k'}. \tag{15}$$

Note that the CFL-condition (14) is slightly more restrictive than the one in [3]. For example, for $\theta = 1$ we obtain $C_1 = 1/\sqrt{3} - 1/2 \approx 0.077$, as opposed to $C_1 = (\sqrt{7} - 2)/6 \approx 0.1076$ for the NT2d scheme. For $\theta = 2$, $C_2 = 0$, as in [3].

Let us now revisit the radially symmetric Sod problem discussed above and recompute the approximate solution using LN2d with exactly the same parameters as in Figure 1.

Figure 4 shows a scatter plot of the corresponding solution at time $t = 0.2$. Now, most of the directional effects have disappeared, in particular the overshoots in pressure and radial velocity immediately behind the leading shock.

TABLE 1. *Runtime and L^1-errors for the NT2d and LN2d runs corresponding to Figures 1 and 4.*

	ρ	ρu_r	E	p	u_r	CPU
Figure 1 (NT2d)	2.391e-02	1.857e-02	4.450e-02	4.854e-02	1.804e-02	6.0
Figure 4 (LN2d)	2.313e-02	1.725e-02	4.179e-02	4.683e-02	1.715e-02	9.2

Table 1 gives L^1-errors and runtimes for the two computations. The errors are computed relative to the cell average projection of an accurate front tracking solution of the corresponding reduced one-dimensional, inhomogeneous problem.

Finally, we include a study of the accuracy of LN2d for two different problems with smooth solutions and make comparisons with NT2d. For each problem we use periodic boundary conditions and compute the error on a series of refined grids using fixed CFL number 0.3. The first example is an oblique, linear advection $u_t+u_x+u_y = 0$ with initial data $\sin(\pi(x+y))$ as in [3]. The error is measured at time $t = 2.0$. The second example is the Euler equations on the unit square subject to initial conditions $(\rho, u, v, p) = \big(1 + 0.1\cos(2\pi x)\cos(2\pi y), cos(\theta), \sin(\theta), 1\big)$ for $\theta = 0.1\pi$. The error in ρ is measured at time $t = 0.5$.

Table 2 shows the results of the grid refinement study. The improved flux quadrature decreases the errors and improves the convergence rates at the cost of a moderate increase in the runtime. The increase is larger for the Euler equations due to the more costly flux evaluations. The convergence rates confirm that LN2d is (at least) second-order accurate for these two examples.

4. Concluding Remarks

We have demonstrated how one can increase the number of propagation directions in a two-dimensional central difference scheme by a careful design of the quadrature rule used in the numerical flux computation. The new quadrature rule improves the accuracy of the scheme for smooth solutions and reduces grid-orientation effects for radially symmetric solutions with strong shocks.

References

[1] H. Nessyahu and E. Tadmor. Non-oscillatory central differencing for hyperbolic conservation laws. *J. Comput. Phys.* 87:408–463, 1990.

[2] P. Arminjon, D. Stanescu and M.-C. Viallon. A two-dimensional finite volume extension of the Lax–Friedrichs and Nessyahu-Tadmor schemes for compressible flows. *Proc. 6th. Int. Symp. on CFD, Lake Tahoe* M. Hafez and K. Oshima (eds.) , Vol. IV, pp. 7–14, 1995.

[3] G.-S. Jiang and E. Tadmor. Nonoscillatory central schemes for multidimensional hyperbolic conservation laws. *SIAM J. Sci. Comput.* 19(6):1892–1917 (electronic), 1998.

TABLE 2. *L^1-errors, ratio of runtimes (τ=runtime(LN2d)/runtime(NT2d)), and average convergence rates for the two refinement studies on a series of $N \times N$ grids.*

	scalar			Euler		
N	LN2d	NT2d	τ	LN2d	NT2d	τ
40	1.137e-01	9.780e-02	1.23	2.642e-03	2.737e-03	1.61
80	2.893e-02	2.653e-02	1.23	4.004e-04	4.428e-04	1.54
160	6.124e-03	6.782e-03	1.23	3.273e-05	5.059e-05	1.52
320	8.052e-04	1.552e-03	1.23	3.548e-06	9.412e-06	1.57
rate	2.38	1.99	—	3.18	2.73	—

(Knut–Andreas Lie) SINTEF Applied Mathematics, P.O. Box 124 Blindern, N–0314 Oslo, Norway. Also: Department of Informatics, University of Oslo

E-mail address: `Knut-Andreas.Lie@math.sintef.no`

URL: `http://www.ifi.uio.no/~kalie/`

(Sebastian Noelle) Institut für Geometrie und Praktische Mathematik, RWTH Aachen, D-52056 Aachen, Germany

E-mail address: `noelle@igpm.rwth-aachen.de`

URL: `http://www.igpm.rwth-aachen.de/~noelle/`